

Closure to “Computational Analysis for Mixed Convective Flows of Viscous Fluids With Nanoparticles” (Farooq, U., Lu, D. C., Ahmed, S., and Ramzan, M., 2019, ASME J. Therm. Sci. Eng. Appl., 11(2), p. 021013)

Jifeng Cui¹

College of Science,
Inner Mongolia University of Technology,
Hohhot 010051, China
e-mail: cjf@imut.edu.cn

Umer Farooq

Department of Mathematics,
COMSATS University Islamabad,
Park Road Chak Shahzad,
Islamabad 44000, Pakistan
e-mail: umer_farooq@comsats.edu.pk

Raheela Razzaq

Department of Mathematics,
COMSATS University Islamabad,
Park Road Chak Shahzad,
Islamabad 44000, Pakistan
e-mail: raheelarazzaq1@gmail.com

Waseem Asghar Khan

Department of Mathematics,
College of Sciences AlZulfi,
Majmaah University,
Al Majma'ah 11952, Saudi Arabia
e-mail: wa.khan@mu.edu.sa

Mogtaba Ahmed Yousif

Department of Mathematics,
College of Sciences AlZulfi,
Majmaah University,
Al Majma'ah 11952, Saudi Arabia
e-mail: Mogatab.m@mu.edu.sa

The authors regret in the published paper referenced above and agree with the discussion by Pantokratoras (2019, “Discussion: “Computational Analysis for Mixed Convective Flows of Viscous Fluids With Nanoparticles” (Farooq, U., Lu, D. C., Ahmed, S., and Ramzan, M., 2019, ASME J. Therm. Sci. Eng. Appl., 11(2), p. 021013),” ASME J. Therm. Sci. Eng. Appl., 11(5), p. 055503). In this Closure, the non-similar mathematical model is developed to describe the mixed convective nanofluid flow over vertical sheet which is stretching at an exponential rate. In the published article referenced above, similarity transformations are utilized to convert the governing nonlinear partial differential equations (PDEs) into ordinary differential equations (ODEs). The important physical numbers such as magnetic field (M^2), Brownian motion parameter (N_b), thermophoresis (N_t), Eckert number (Ec), ratio of mass transfer Grashof to heat transfer Grashof (N), buoyancy parameter (λ), and

*Reynolds number (Re) appearing in the dimensionless ODEs are still functions of coordinate “ x ”; therefore, the problem is non-similar. In this corrigendum, the non-similar model is developed by using $\xi(x)$ as non-similarity variable and $\eta(x, y)$ as pseudo-similarity variable. The dimensionless non-similar model is numerically simulated by employing local non-similarity via *bvp4c*. The graphical results show no change in behavior. The important thermal and mass transport quantities such as Nusselt number and Sherwood number have been computed for the non-similar model, and results are compared with the published article.*

[DOI: 10.1115/1.4050572]

Keywords: non-similar modeling, mixed convection, exponentially stretching surface, *bvp4c*, heat and mass transfer, magnetohydrodynamic (MHD)

1 Introduction

In the literature, most of the boundary layer problems have been tackled using similarity transformations which change the governing partial differential equations (PDEs) to ordinary differential equations (ODEs) [1,2]. Numerical and analytical methods are generally used to evaluate these ODEs. Analytical methods are mostly used to solve similar flows due to calculation and ideal simplicity. Sometimes it may happen that after applying similarity variables, the physical parameters in the governing equations are still functions of coordinate “ x ” (see Refs. [3,4]), and these problems are known as non-similar. Despite of this fact that non-similar flows are extensive in nature and they have vast applications in real life, there are still lesser publications in this direction compared with similar flows. Many numerical techniques have been developed which can tackle non-similar flows. The most prominent technique is known as local non-similarity established by Sparrow et al. [5]. In this corrigendum, local non-similarity via *bvp4c* is employed. The main drawback of the local similarity approach is that it neglects the non-similar part. To overcome this drawback, Sparrow and Yu [6] presented a new technique termed as “method of local non-similarity” to obtain results for non-similar flows. Later non-similar flows were studied by numerous authors (see for instance, Refs. [5,7–11]). In this corrigendum, non-similar transformations have been proposed for mixed convective boundary layer flow over vertical surface which is stretching at an exponential rate. The local non-similarity technique via *bvp4c* is employed to obtain non-similar solutions.

2 Mathematical Formulation

Consider two-dimensional, laminar, incompressible magnetized nanofluid flow which is produced by the exponential expansion of the sheet with velocity “ U_w ”. The buoyancy in terms of temperature and concentration is incorporated in the momentum equation. The impacts of magnetic and viscous dissipations are incorporated in the energy equation. The physical interpretation of the model is described as follows:

$$\frac{\partial u}{\partial x} + \frac{\partial v}{\partial y} = 0 \quad (1)$$

$$u \frac{\partial u}{\partial x} + v \frac{\partial u}{\partial y} = \nu \left(\frac{\partial^2 u}{\partial y^2} \right) - \frac{\sigma B_o^2}{\nu_f} u + g\beta_c(C - C_\infty) + g\beta_T(T - T_\infty) \quad (2)$$

$$u \frac{\partial T}{\partial x} + v \frac{\partial T}{\partial y} = \alpha \left(\frac{\partial^2 T}{\partial y^2} \right) + \frac{\mu}{\rho_f C_p} \left(\frac{\partial u}{\partial y} \right)^2 + \tau D_B \left(\frac{\partial C}{\partial y} \frac{\partial T}{\partial y} \right) + \frac{\tau D_T}{T_\infty} \left(\frac{\partial T}{\partial y} \right)^2 + \frac{\sigma B_o^2}{C_p \rho_f} u^2 \quad (3)$$

¹Corresponding author.

Manuscript received January 4, 2021; final manuscript received March 9, 2021; published online April 19, 2021. Assoc. Editor: Sandip Mazumder.

$$u \frac{\partial C}{\partial x} + v \frac{\partial C}{\partial y} = D_B \left(\frac{\partial^2 C}{\partial y^2} \right) + \frac{D_T}{T_\infty} \left(\frac{\partial^2 T}{\partial y^2} \right) \quad (4)$$

In preceding expressions, u and v represent velocities in x - and y -directions, and α , ν , T , σ , C_p , T_∞ , D_B , C , D_T , and ρ_f represent thermal diffusivity, kinematic viscosity, temperature, electrical conductivity, specific heat, freestream temperature, Brownian diffusion coefficient, nanoparticle volume fraction, thermophoretic diffusion coefficient, and fluid density, respectively.

The relevant conditions take the following forms:

$$\text{At } y = 0, \quad u = U_w(x) = U_0 \exp\left(\frac{x}{l}\right), \quad v = 0, \quad C = C_w(x),$$

$$-k \frac{\partial T}{\partial y} = h_f (T_w - T) \quad (5)$$

$$\text{As } y \rightarrow \infty, \quad v \rightarrow 0, \quad u \rightarrow 0, \quad T \rightarrow T_\infty, \quad C \rightarrow C_\infty \quad (6)$$

where

$$T_w = T_\infty + T_0 \exp\left(\frac{2x}{l}\right), \quad C_w = C_\infty + C_0 \exp\left(\frac{2x}{l}\right)$$

In earlier mentioned conditions, C_w and T_w are the concentration and temperature on the wall and h_f is the convective heat transfer coefficient. Introducing two dimensionless numbers

ξ and η the non-similarity variable and pseudo-similarity variable, respectively, non-similarity transformations are then proposed as

$$\left\{ \begin{array}{l} \xi = \exp\left(\frac{x}{l}\right), \quad \eta = \sqrt{\frac{U_0}{2\nu l}} y \exp\left(\frac{x}{2l}\right) \\ u = U_0 \frac{\partial f}{\partial \eta}(\xi, \eta) \exp\left(\frac{x}{l}\right) \\ v = -\sqrt{\frac{\nu U_0}{2l}} \exp\left(\frac{x}{2l}\right) \left(f(\xi, \eta) + \eta \frac{\partial f}{\partial \eta} + 2\xi \frac{\partial f}{\partial \xi} \right) \\ T = \theta(\xi, \eta)(T_w - T_\infty) + T_\infty \\ C = \phi(\xi, \eta)(C_w - C_\infty) + C_\infty \end{array} \right. \quad (7)$$

Using Eq. (7) in Eqs. (1)–(6), they are transformed as follows:

$$\begin{aligned} \frac{\partial^3 f}{\partial \eta^3} + f \frac{\partial^2 f}{\partial \eta^2} - 2 \left(\frac{\partial f}{\partial \eta} \right)^2 - 2M^2 \xi^{-1} \frac{\partial f}{\partial \eta} + 2\lambda(\theta + N\phi) \\ = 2\xi \left(\frac{\partial f}{\partial \eta} \frac{\partial^2 f}{\partial \xi \partial \eta} - \frac{\partial^2 f}{\partial \eta^2} \frac{\partial f}{\partial \xi} \right) \end{aligned} \quad (8)$$

$$\frac{\partial^2 \theta}{\partial \eta^2} + \text{Pr} \left(f \frac{\partial \theta}{\partial \eta} - 4\theta \frac{\partial f}{\partial \eta} + 2M^2 \text{Ec} \xi^{-1} \left(\frac{\partial f}{\partial \eta} \right)^2 + \xi^2 \left(N_b \frac{\partial \phi}{\partial \eta} \frac{\partial \theta}{\partial \eta} + N_t \left(\frac{\partial \theta}{\partial \eta} \right)^2 \right) + \text{Ec} \left(\frac{\partial^2 f}{\partial \eta^2} \right)^2 \right) = 2\text{Pr} \xi \left(\frac{\partial f}{\partial \eta} \frac{\partial \theta}{\partial \xi} - \frac{\partial \theta}{\partial \eta} \frac{\partial f}{\partial \xi} \right) \quad (9)$$

$$\frac{\partial^2 \phi}{\partial \eta^2} + \frac{N_t}{N_b} \frac{\partial^2 \theta}{\partial \eta^2} - \text{Sc} \left(4\phi \frac{\partial f}{\partial \eta} - f \frac{\partial \phi}{\partial \eta} \right) = 2\text{Sc} \xi \left(\frac{\partial f}{\partial \eta} \frac{\partial \phi}{\partial \xi} - \frac{\partial \phi}{\partial \eta} \frac{\partial f}{\partial \xi} \right) \quad (10)$$

The boundary conditions are as follows:

$$\begin{aligned} \frac{\partial f}{\partial \eta}(\xi, 0) = 1, \quad f(\xi, 0) + 2\xi \frac{\partial f}{\partial \xi}(\xi, 0) = 0, \quad \phi(\xi, \infty) = 0, \quad \theta(\xi, 0) = 1 \\ \frac{\partial f}{\partial \eta}(\xi, \infty) = 0, \quad \theta(\xi, \infty) = 0, \quad \frac{\partial \theta}{\partial \eta}(\xi, 0) = -\gamma \xi^{-1/2} (1 - \theta(\xi, 0)) \end{aligned} \quad (11)$$

The parameters Re , λ , N_b , Pr , N_t , M , Le , N , and Ec represent Reynolds number, buoyancy parameter, Brownian motion, Prandtl number, thermophoresis, magnetic field, Lewis number, ratio between mass transfer Grashof number and heat transfer Grashof number, and Eckert number, respectively. The dimensionless parameters are represented as

$$\begin{aligned} \lambda = \frac{\text{Gr}}{\text{Re}^2}, \quad \text{Pr} = \frac{\nu}{\alpha}, \quad N_b = \frac{\tau D_B C_0}{\nu}, \quad N_t = \frac{\tau T_0 D_T}{\nu T_\infty}, \quad M^2 = \frac{\sigma B_0^2 l}{\rho_f U_0}, \quad \text{Ec} = \frac{U_0^2}{C_p T_0}, \quad \text{LePr} = \text{Sc} \\ \text{Sc} = \frac{\nu}{D_B}, \quad \text{Re} = \frac{l U_0}{\nu}, \quad N = \frac{\text{Gr}^*}{\text{Gr}}, \quad \gamma = \frac{h_f}{k} \sqrt{\frac{2\nu l}{U_0}}, \quad \text{Gr} = \frac{g \beta_T T_0 l^3}{\nu^2}, \quad \text{Gr}^* = \frac{g \beta_c C_0 l^3}{\nu^2} \end{aligned} \quad (12)$$

The local Nusselt number, skin friction, and local Sherwood number coefficients are

$$\text{Nu} = \frac{x q_l}{k(T_1 - T_\infty)}, \quad C_f = \frac{2\tau_l}{\rho U_l^2}, \quad \text{Sh} = \frac{x j_l}{D_B(C_l - C_\infty)} \quad (13)$$

where j_l is the mass flux, τ_l is the wall skin friction, and q_l is heat flux from surface, defined below:

$$\tau_l = \mu \left(\frac{\partial u}{\partial y} \right)_{y=0}, \quad j_l = -D_B \left(\frac{\partial C}{\partial y} \right)_{y=0}, \quad q_l = -k \left(\frac{\partial T}{\partial y} \right)_{y=0} \quad (14)$$

$$\begin{aligned} (2\text{Re})^{(1/2)} C_f = \sqrt{2} f''(\xi, 0), \\ \text{Re}^{-(1/2)} \text{Sh} = -\sqrt{\frac{1}{2}} \ln(\xi) \phi'(\xi, 0), \\ \text{Re}^{-(1/2)} \text{Nu} = -\sqrt{\frac{1}{2}} \theta'(\xi, 0) \ln(\xi) \end{aligned} \quad (15)$$

3 Non-Similarity Method

To interpret several non-similarity boundary layers, many scientists utilize this method (see for instance, Refs. [12–14]). The principle of local similarity is usually considered for outcomes of non-similarity boundary layer. With the help of the local non-similar technique, we have approximated non-similar PDEs through ODEs. In this method, the right-edge of Eqs. (8)–(10) are supposed to be sufficiently small; therefore, it can be estimated to

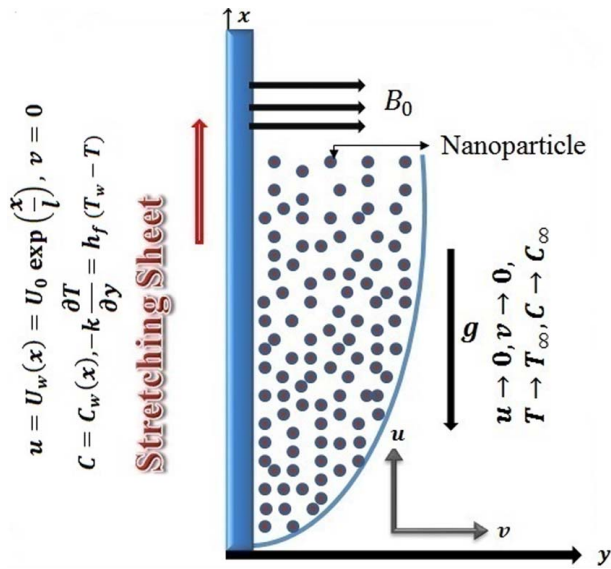


Fig. 1 Physical configuration

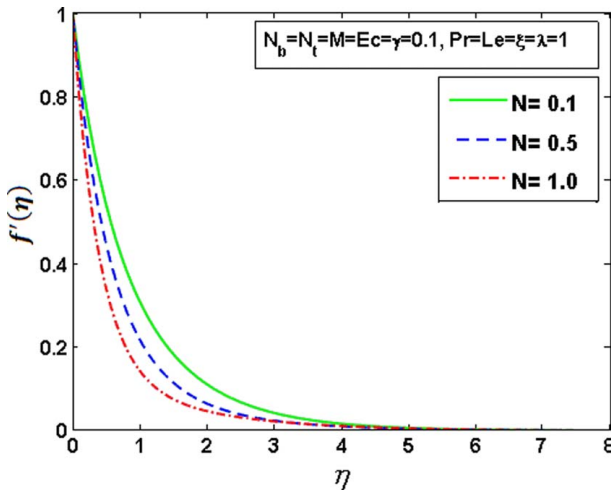


Fig. 2 Graph of $f'(\eta)$ for distinct values of N

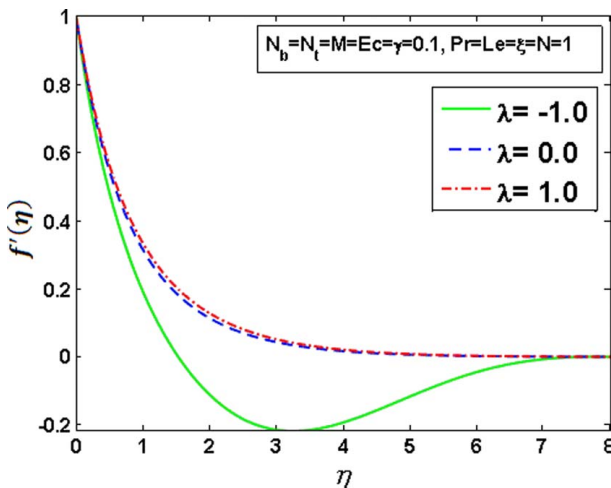


Fig. 3 Graph of $f'(\eta)$ for distinct values of λ

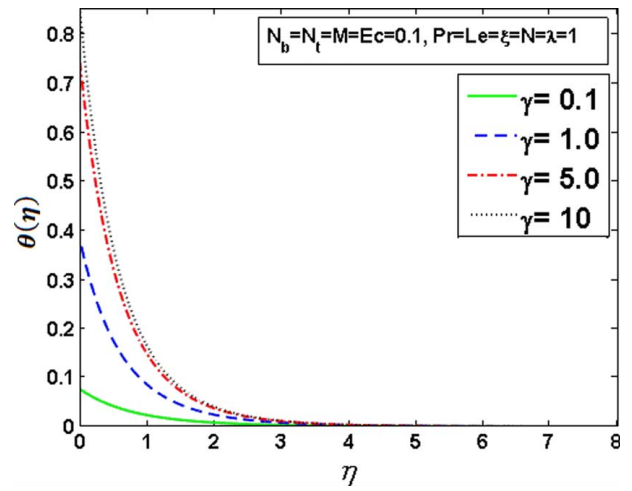


Fig. 4 Graph of $\theta(\eta)$ for distinct values of γ

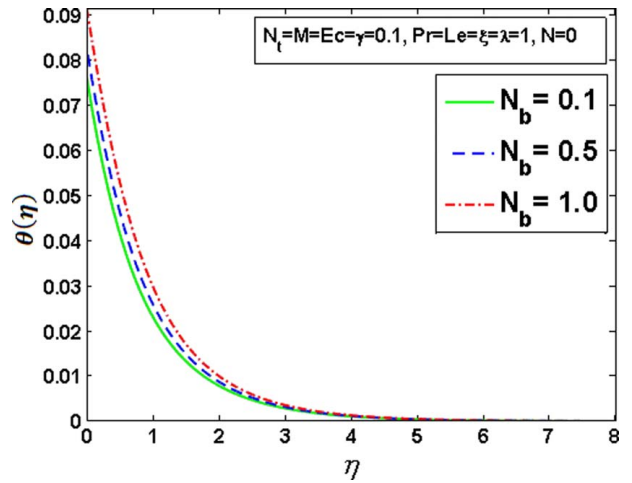


Fig. 5 Graph of $\theta(\eta)$ for distinct values of N_b

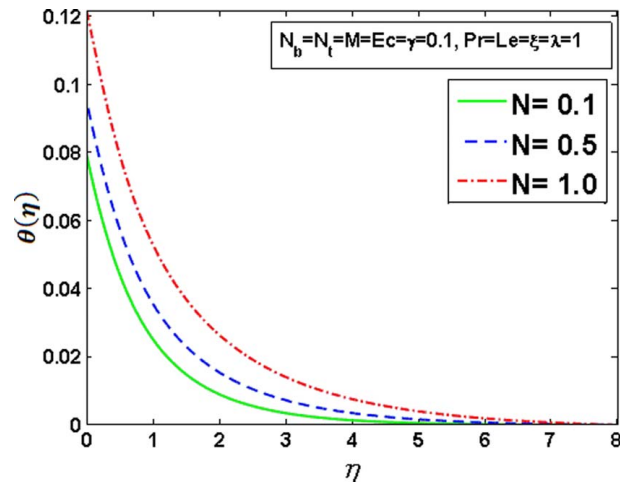


Fig. 6 Graph of $\theta(\eta)$ for distinct values of N

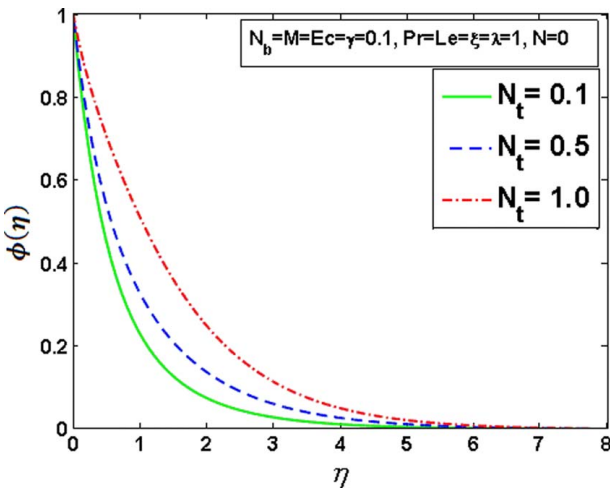


Fig. 7 Graph of $\phi(\eta)$ for distinct values of N_t

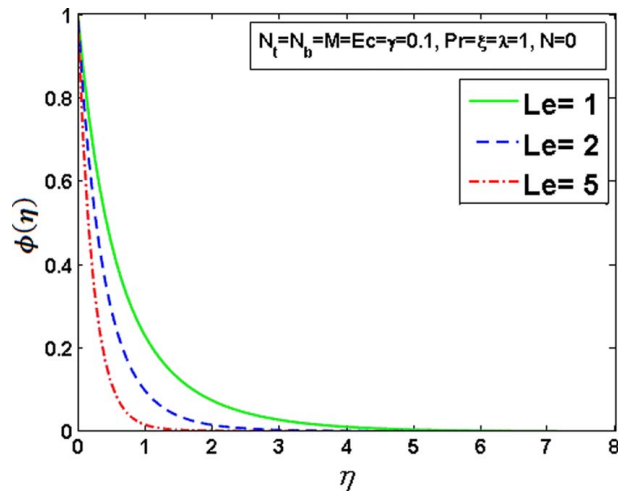


Fig. 10 Graph of $\phi(\eta)$ for distinct values of Le

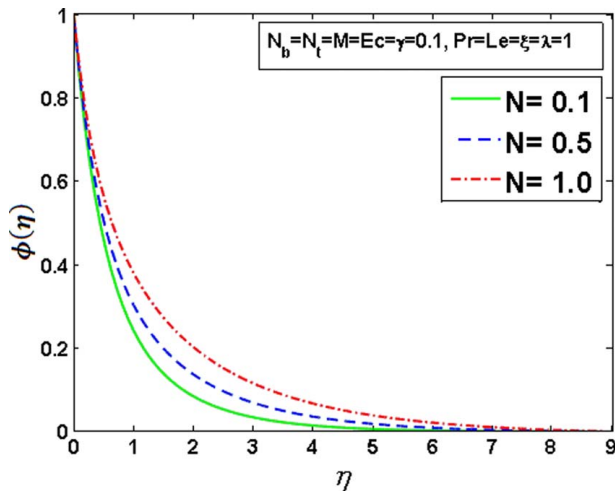


Fig. 8 Graph of $\phi(\eta)$ for distinct values of N

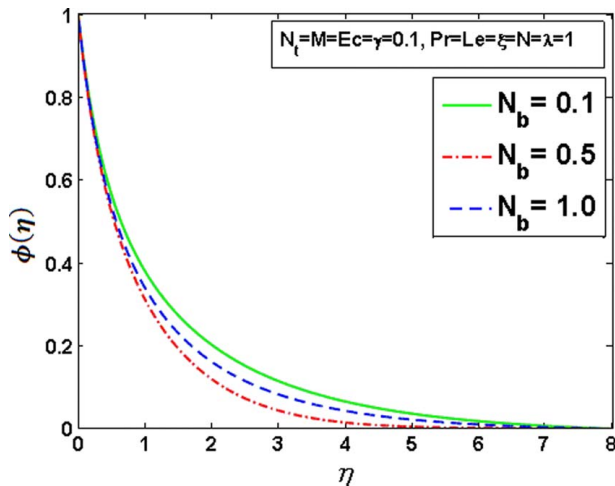


Fig. 9 Graph of $\phi(\eta)$ for distinct values of N_b

zero, and hence leading PDEs become ODEs. The final resulting non-dimensional set of coupled nonlinear PDEs is then resolved with the utilization of `bvp4c` function in `MATLAB`. A technique for finding locally non-similar boundary layer is discussed and demonstrated by Farooq et al. [15].

4 Results and discussion

Local non-similarity via `bvp4c` is utilized for the influences of numerous parameters on temperature profile θ , velocity profile f' , and concentration profile ϕ . Figures 1–10 are generated for distinct values of γ , N , N_b , N_t , λ , and Le . The graphs depict similar behavior to the original problem [16].

Tables 1–3 present the comparison between local similar skin friction, Nusselt and Sherwood numbers of Farooq et al. [16] and present non-similar results.

Table 1 Comparison of local similar and non-similar C_{fx} (local skin friction) for different values of λ versus N when $M = Ec = N_b = \gamma = N_t = 0.1$, $\xi = Sc = 1$, $Pr = 3$

| Parameters | Farooq et al. [16] | | Present | Difference (%) | |
|------------|--------------------|-----|---------------|----------------|-------------------------|
| | λ | N | | | $C_{fx} (Re_x^{(1/2)})$ |
| 1 | 1 | 1 | -0.4909596405 | -0.6647215909 | 26.14 |
| | 2 | 2 | 0.1349248240 | -0.1404157755 | 196.08 |
| | 3 | 3 | 0.7207345529 | 0.3502839440 | 105.75 |
| 2 | 1 | 1 | 0.1691179725 | -0.1207441687 | 240.06 |
| | 2 | 2 | 1.3206151204 | 0.8362957739 | 57.91 |
| | 3 | 3 | 2.4177911886 | 1.7301144394 | 39.74 |

Table 2 Comparison of local similar and non-similar Nu (local Nusselt number) for different values of N_b versus Ec when $Pr = 3$, $N_t = M = 0.1$, $N = \lambda = Sc = \xi = \gamma = 1$

| Parameters | Farooq et al. [16] | | Present | Difference (%) | |
|------------|--------------------|-------|---------------|----------------|--------------------|
| | Ec | N_b | | | $Nu (Re_x^{-1/2})$ |
| 1 | 0.1 | 0.1 | -0.5659884824 | -0.3587657268 | 57.75 |
| | 0.2 | 0.2 | -0.5433373428 | -0.3413113332 | 59.19 |
| | 0.3 | 0.3 | -0.5260558981 | -0.3335272975 | 57.71 |
| 2 | 0.1 | 0.1 | -0.5594207277 | -0.1566273066 | 257.16 |
| | 0.2 | 0.2 | -0.5080076972 | -0.1506193302 | 237.27 |
| | 0.3 | 0.3 | -0.4827801575 | -0.1455588629 | 231.67 |

Table 3 Comparison of local similar and non-similar Sh (local Sherwood number) for different values of Sc versus N_t when $N_b = Ec = M = \gamma = 0.1, Pr = N = \lambda = \xi = 1$

| Parameters | | Farooq et al. [16] | Present | Difference (%) |
|------------|-------|------------------------|---------------|----------------|
| Sc | N_t | Sh ($Re_x^{-(1/2)}$) | | |
| 3 | 0.1 | -1.8928151531 | -3.0470646222 | 37.88 |
| | 0.3 | -1.5128377645 | -2.9675413434 | 49.02 |
| | 0.5 | -1.1221686851 | -2.8326909229 | 60.38 |
| 5 | 0.1 | -2.5964060620 | -4.1192374623 | 36.96 |
| | 0.3 | -2.3333398044 | -4.0680085443 | 42.64 |
| | 0.5 | -2.0125506640 | -3.9544145612 | 49.10 |

5 Conclusion

The authors agree with the concerns of Pantokratoras [17] on Farooq et al. [16]. Therefore, in this corrigendum, the non-similar model is developed in which the physical parameters are independent of “ x ”. Non-similar solutions depict similar graphical behavior by comparing it with the published article. The important thermal and mass transport quantities such as Nusselt number and Sherwood number have been computed for the non-similar model.

Acknowledgment

This work is supported by the National Natural Science Foundation of China (Approval No.12062018) and the Natural Science Foundation of Inner Mongolia (Approval No. 2018LH01016).

Conflict of Interest

There are no conflicts of interest.

Data Availability Statement

The datasets generated and supporting the findings of this article are obtainable from the corresponding author upon reasonable request. Data provided by a third party are listed in Acknowledgment.

References

- [1] Xu, H., Pop, I., and You, X. C., 2013, “Flow and Heat Transfer in a Nano-Liquid Film Over an Unsteady Stretching Surface,” *Int. J. Heat Mass Transfer*, **60**, pp. 646–652.
- [2] Sreedevi, P., Reddy, P. S., and Chamkha, J. A., 2018, “Magneto-Hydrodynamics Heat and Mass Transfer Analysis of Single and Multi-Wall Carbon Nanotubes Over Vertical Cone With Convective Boundary Condition,” *Int. J. Mech. Sci.*, **135**, pp. 646–655.
- [3] Khan, M. I., Afzal, S., Hayat, T., Waqas, M., and Alsaedi, A., 2020, “Activation Energy for the Carreau-Yasuda Nanomaterial Flow: Analysis of the Entropy Generation Over a Porous Medium,” *J. Mol. Liq.*, **297**, p. 111905.
- [4] Mushtaq, A., Farooq, M. A., Sharif, R., and Razaq, M., 2019, “The Impact of Variable Fluid Properties on Hydromagnetic Boundary Layer and Heat Transfer Flows Over an Exponentially Stretching Sheet,” *J. Phys. Commun.*, **3**(9), p. 95005.
- [5] Sparrow, E. M., Quack, H., and Boerner, C. J., 1970, “Local Non-Similarity Boundary-Layer Solutions,” *AIAA J.*, **8**(11), pp. 1936–1942.
- [6] Sparrow, E. M., and Yu, H. S., 1971, “Local Non-Similarity Thermal Boundary Layer Solutions,” *ASME J. Heat Transfer*, **93**(4), pp. 328–334.
- [7] Massoudi, M., 2001, “Local Non-Similarity Solutions for the Flow of Non-Newtonian Fluid Over a Wedge,” *Int. J. Non-Linear Mech.*, **36**(6), pp. 961–976.
- [8] Muhaimin, I., and Kandasamy, R., 2010, “Local Nonsimilarity Solution for the Impact of a Chemical Reaction in an MHD Mixed Convection Heat and Mass Transfer Flow Over a Porous Wedge in the Presence of Suction/Injection,” *ASME J. Appl. Mech. Tech. Phys.*, **51**(5), pp. 721–731.
- [9] Farooq, U., Hayat, T., Alsaedi, A., and Liao, S. J., 2015, “Series Solutions of Non-Similarity Boundary Layer Flows of Nano-Fluids Over Stretching Surfaces,” *Numer. Algor.*, **70**, pp. 43–59.
- [10] Akgül, M. B., and Pakdemirli, M., 2012, “Magneto-hydrodynamic and Slip Effects on the Flow and Mass Transfer Over a Microcantilever-Based Sensor,” *J. Appl. Math.*, **2012**, pp. 1–11.
- [11] Srinivasacharya, D., and Surender, O., 2014, “Non-Similar Solution for Natural Convective Boundary Layer Flow of a Nanofluid Past a Vertical Plate Embedded in a Doubly Stratified Porous Medium,” *Int. J. Heat Mass Transfer*, **71**, pp. 431–438.
- [12] Raees, A., Farooq, U., Hussain, M., Khan, W. A., and Farooq, F. B., 2021, “Non-Similar Mixed Convection Analysis for Magnetic Flow of Second Grade Nano-Fluid Over Vertically Stretching Sheet,” *Commun. Theor. Phys.*
- [13] Abdullah, A. A., Ibrahim, F. S., and Chamkha, J. A., 2018, “Non-Similar Solution of Unsteady Mixed Convective Flow Near the Stagnation Point of a Heated Vertical Plate in a Porous Medium Saturated With a Nano-Fluid,” *J. Por. Media*, **21**(4), pp. 363–388.
- [14] Mureithi, E. W., and Mason, D. P., 2010, “Local Non-Similarity Solutions for a Forced-Free Boundary Layer Flow With Viscous Dissipation,” *Math. Comput. Appl.*, **15**(4), pp. 558–573.
- [15] Farooq, U., Ijaz, M. A., Khan, M. I., and Liao, S. J., 2020, “Modeling and Non-Similar Analysis for Darcy-Forchheimer-Brinkman Model of Casson Fluid in a Porous Media,” *Int. Commun. Heat Mass Transfer*, **119**, p. 104955.
- [16] Farooq, U., Lu, D., Ahmed, S., Ramzan, M., Chung, J. D., and Chandio, F. A., 2019, “Computational Analysis for Mixed Convective Flows of Viscous Fluids With Nanoparticles,” *ASME J. Therm. Sci. Eng. Appl.*, **11**(2), p. 021013.
- [17] Pantokratoras, A., 2019, “Discussion: “Computational Analysis for Mixed Convective Flows of Viscous Fluids With Nanoparticles” (Farooq, U., Lu, D. C., Ahmed, S., and Ramzan, M., 2019, *ASME J. Therm. Sci. Eng. Appl.*, **11**(2), p. 021013),” *ASME J. Therm. Sci. Eng. Appl.*, **11**(5), p. 055503.